

REGULAR PAPER

# Pressure dependence of Poisson's ratio of glassy Baltic amber studied by Brillouin scattering spectroscopy

To cite this article: Sergey N. Tkachev *et al* 2021 *Jpn. J. Appl. Phys.* **60** SDDA04

View the [article online](#) for updates and enhancements.



# Pressure dependence of Poisson's ratio of glassy Baltic amber studied by Brillouin scattering spectroscopy

Sergey N. Tkachev<sup>1</sup>, Muhtar Ahart<sup>2</sup>, Vladimir N. Novikov<sup>3</sup>, and Seiji Kojima<sup>4\*</sup> 

<sup>1</sup>Center for Advanced Radiation Sources, University of Chicago, Chicago, IL 60637, United States of America

<sup>2</sup>Department of Physics, University of Illinois at Chicago, Chicago, IL 60609, United States of America

<sup>3</sup>Institute of Automation and Electrometry, Russian Academy of Sciences, Novosibirsk, 630090, Russia

<sup>4</sup>Faculty of Pure and Applied Sciences, University of Tsukuba, Tsukuba, Ibaraki 305-8573, Japan

\*E-mail: [kojima@ims.tsukuba.ac.jp](mailto:kojima@ims.tsukuba.ac.jp)

Received December 1, 2020; revised February 2, 2021; accepted February 26, 2021; published online March 17, 2021

Amber is a typical natural glass with very long aging time. Elastic properties of amber at high pressures have been studied using Brillouin scattering and a diamond anvil cell. Both longitudinal and transverse acoustic modes have been observed up to 12 GPa. The pressure dependences of longitudinal, shear, Young's, and bulk moduli, compressibility, and Poisson's ratio were determined. The longitudinal, shear, Young's, bulk moduli show the remarkable increase, and compressibility shows a marked decrease with increasing pressure. However, it is found that the pressure dependence of Poisson's ratio is very small. The mechanism of this small pressure dependence was discussed. The Cauchy type relation between longitudinal and shear moduli was examined. Its coefficients show the deviation from the Cauchy relation owing to the coexistence of different intermolecular interactions in amber. © 2021 The Japan Society of Applied Physics

## 1. Introduction

The magnitude of the elastic moduli is governed by both the atomic bond energy and the atomic packing density, while the Poisson's ratio is related to the degree of symmetry of the structural units existing at the molecular scale. The pressure dependence of these properties are very important, because the pressure drastically shortens the interatomic distance and density. Fragility of liquids is defined as  $E/(T_g \ln 10)$  where  $E$  is the apparent activation energy of shear viscosity  $\eta$  or structural relaxation time  $\tau_\alpha$  at the glass transition temperature  $T_g$ . The fragility index  $m$  of a glass-forming liquid is intimately linked to a very basic property of the corresponding glassy states: Poisson's ratio, or the ratio of longitudinal and transverse sound velocity,  $V_L$  and  $V_T$ , respectively.<sup>1)</sup> Analysis of a large number of glasses, including covalent and hydrogen-bonded, van-der-Waals and ionic glasses, shows a correlation between  $V_L/V_T$  and  $m$ . The relation between Poisson's ratio and  $m$  has attracted attention.<sup>2)</sup>

Regarding pressure dependence of fragility, it was reported that three kinds of intermediate small-molecule glass-formers do not show a pressure dependence of fragility within experimental error.<sup>3)</sup> The defect diffusion model (DDM) explains these experimental findings, supporting a clustering mechanism in the glass-forming process.

The pressure dependence of Poisson's ratio of a typical strong glass, SiO<sub>2</sub> shows the remarkable increase up to 13 GPa.<sup>4)</sup> However, in the intermediate glycerol, at low pressure it increases gradually, while at pressure higher than 1 GPa it becomes constant.<sup>5)</sup> Although pressure dependences of the Poisson's ratio have been studied for few glass-forming systems, not much is known about the influence of pressure on Poisson's ratio.

In many polymer glasses, the fragility increases as molecular weight increases. Amber is a unique example of a glass that has been aging for a very long time below its glass transition temperature, thus reaching a state which is not accessible under normal experimental conditions.<sup>6)</sup> Density, melting temperature, and refractive index of Baltic amber are

1.0–1.1 g cm<sup>-3</sup>, 250 °C–300 °C, and 1.54, respectively. Main part of Baltic Amber is a polymer of the labdatrienoid compounds including communic acid and communal with its hydroxyl groups partially succinylated. In addition, it contains a few percent of many other compounds such as terpinol, succinate and hemisuccinate esters.<sup>7)</sup>

It is very fragile and its fragility index was reported to be about 90.<sup>8)</sup> As fragility increases, the intensity of fast relaxation process increases while the intensity of boson peak decreases. The boson peak of Baltic amber is not yet observed by Raman scattering and THz time domain spectroscopy reflecting the very high fragility index.<sup>9)</sup> Recently amber has attracted much attention as an ideal fragile glass.<sup>10)</sup> In the present study the pressure dependence of elastic properties of Baltic amber is investigated by Brillouin scattering.

## 2. Experimental methods

Baltic Amber is fossil pine resin of the Eocene Period and is about 40 million years old. The Baltic amber imported from Lithuania was purchased from Crystal World Co., Ltd., and it was used without any thermal treatment. Brillouin scattering spectra of Baltic amber were measured in a symmetric scattering geometry, with the scattering angle of 50 degree, using a high-contrast 3 + 3 passes tandem Fabry–Perot interferometer with a free spectral range of 25 GHz for longitudinal acoustic (LA) and transverse acoustic (TA) modes.<sup>11)</sup> The exciting source was a diode-pumped solid state laser with a wavelength of 532 nm. The pressure dependence was measured using a symmetric diamond anvil cell.<sup>12)</sup> The schematic illustration of scattering geometry for DAC is shown in Fig. 1(a). The relation among wavevectors of incident light  $\vec{k}_i$ , scattered light  $\vec{k}_s$ , and acoustic phonon  $\vec{q}$  are shown in Fig. 1(b). A piece of amber glass sample was grounded first, then loaded into a 150  $\mu$ m stainless steel gasket hole. The pressure of a sample was determined by the standard Ruby fluorescence method. No pressure medium was added.<sup>13)</sup> Both compression and decompression curves were measured between ambient and 12 GPa. Brillouin

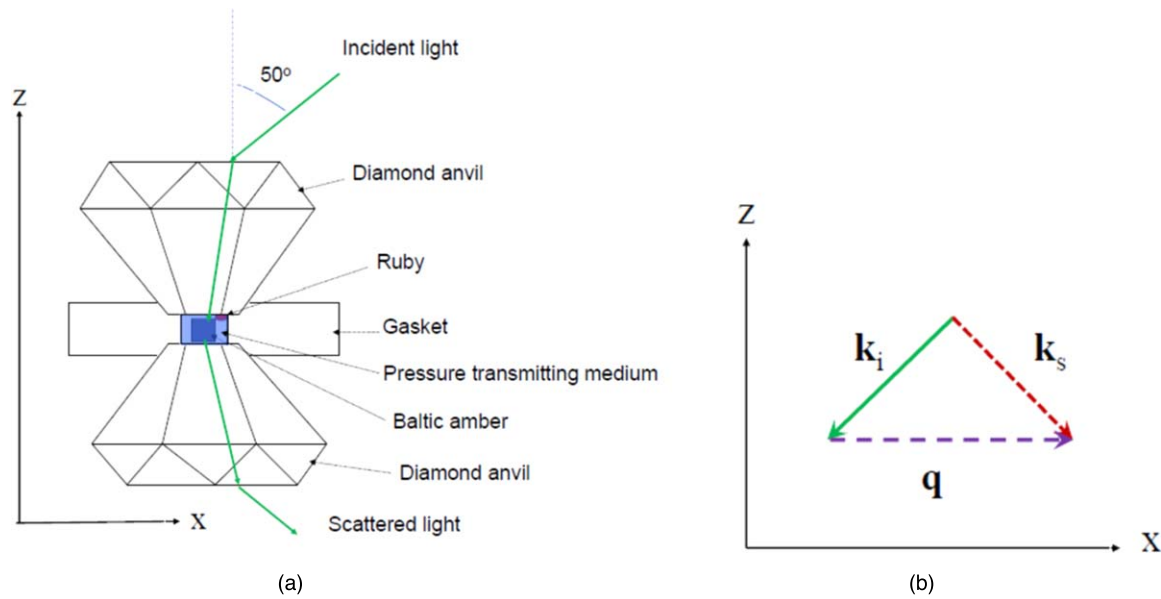


**Fig. 1.** (Color online) (a) Schematic illustration of Brillouin scattering experiment at high pressures using a diamond anvil cell. (b) The relation of wavevectors among incident, scattered light beams, and acoustic phonon.

scattering experiments were performed at Sector-13 of APS, Argonne National Laboratory.<sup>14)</sup>

### 3. Results and discussion

#### 3.1. Brillouin scattering and elastic properties

The pressure dependence of Brillouin scattering spectra of Baltic amber is shown in Fig. 2(a). The intensity of the TA mode is much weaker than that of the LA mode. Up to the present, there is no report on the observation of the TA mode of Baltic amber within our knowledge, while the TA peaks were clearly observed as shown in Fig. 2(b).<sup>13)</sup> The pressure dependence of LA and TA frequency shifts is shown in Fig. 3. The sound velocity  $V$  is determined by the frequency shift  $\nu_B$  in a Brillouin scattering spectrum measured in a symmetric scattering geometry using the following equation,

$$V = \frac{\lambda_i \nu_B}{2 \sin \frac{\theta}{2}}. \quad (1)$$

Here,  $\lambda_i$  and  $\theta$  are the wavelength of an incident beam and the scattering angle, respectively.

The pressure dependences of LA and TA velocity are shown in Figs. 4(a) and 4(b), respectively. The pressure dependence of the LA mode velocity  $V_L$  is in a good agreement with the previous study.<sup>15,16)</sup> The LA mode velocity  $V_L$  increases as the pressure  $P$  increases, and it obeys the following empirical equation:

$$V_L = V_0(1 + P/P_0)^n. \quad (2)$$

Here,  $V_0 = 2.70 \text{ km s}^{-1}$ ,<sup>17)</sup>  $P_0 = 0.25 \text{ GPa}$ ,  $n = 0.30$ .

The TA mode velocity  $V_T$  also increases as the pressure  $P$  increases, and it obeys the following empirical equation.

$$V_T = V_0(1 + P/P_0)^k. \quad (3)$$

Here,  $V_0 = 1.39 \text{ km s}^{-1}$ ,  $P_0 = 0.25 \text{ GPa}$ ,  $k = 0.27$ .

Equations (2) and (3) are similar to the pressure dependence of the boson peak frequency  $\nu_{BP}$  predicted in the soft potential model:<sup>18)</sup>

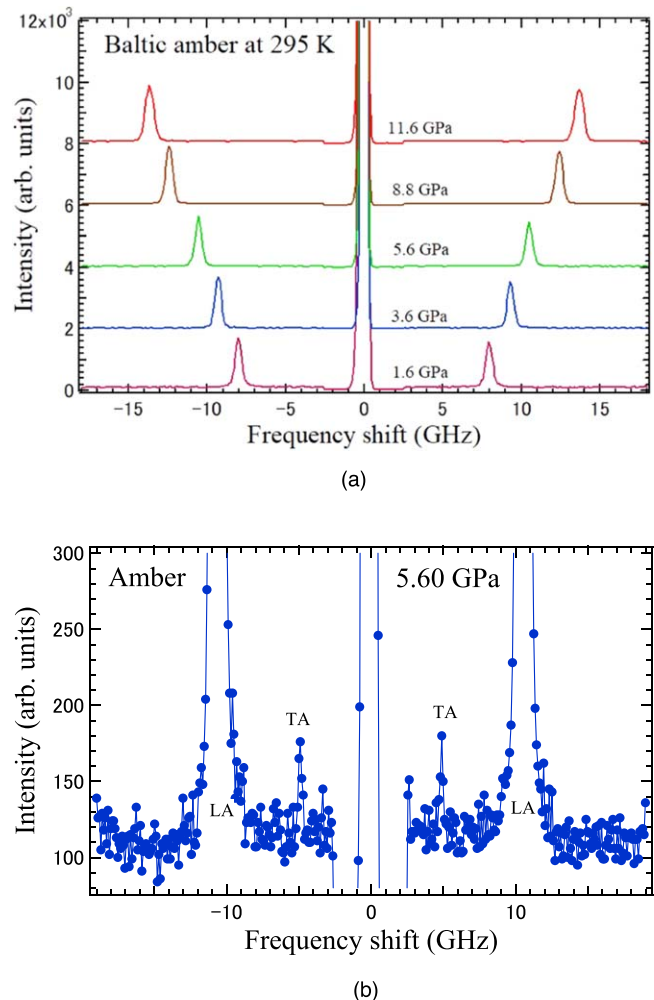


**Fig. 2.** (Color online) (a) Pressure dependence of Brillouin scattering spectra of Baltic amber. (b) Brillouin scattering spectrum of LA and TA frequency shifts of Baltic amber at 5.60 GPa.

$$\nu_{BP} = \nu_0(1 + P/P_0)^{1/3}. \quad (4)$$

The dependence of the type of Eq. (4) is also predicted by a simple model. The relative change of the density with

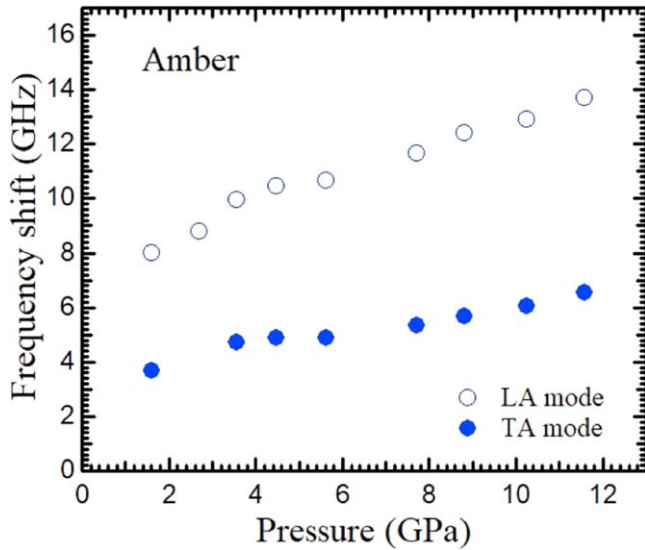


**Fig. 3.** (Color online) Pressure dependence of LA and TA frequency shifts of Baltic amber.

pressure is determined by the bulk modulus  $K$ , which itself depends on pressure:

$$\frac{d \ln \rho}{dP} = 1/K(P). \quad (5)$$

In a good approximation,  $K(P)$  varies linearly with pressure,  $K(P) = K_0 + K_1 P$ . The data of Fig. 5(a) predict  $K_0 = 12.0 \pm 1.6$  GPa,  $K_1 = 5.5 \pm 0.2$ . With this linear dependence of  $K(P)$  we have from Eq. (5)

$$\rho = \rho_0 \left( 1 + \frac{K_1}{K_0} P \right)^{1/K_1}, \quad (6)$$

where  $\rho_0$  is the density at ambient pressure. The change in density leads to the change in the Brillouin frequencies, quantified by the Grüneisen parameter  $\gamma = d \ln \nu / d \ln \rho$ . If one suppose that  $\gamma$  is a constant, using Eq. (6) one has  $\nu_i(P) = \nu_{i0} (\rho(P)/\rho_0)^{\gamma_i}$ , where  $\gamma_i$  ( $i = L, T$ ) is the respective mode Grüneisen parameter. Taking into account Eq. (4), one has

$$\nu_i = \nu_{i0} \left( 1 + \frac{K_1}{K_0} P \right)^{\frac{\gamma_i}{K_1}}. \quad (7)$$

We note that the values of the exponents  $n$  and  $k$  are less than those of polymers which are in the range 0.3–0.38 for the transverse mode and 0.36–0.43 for the longitudinal mode.

For boson peak

$$\nu_{BP} = b \frac{V_T}{L_c}, \quad (8)$$

where  $L_c$  is the structure correlation length, and  $b$  is a parameter of the order of 1. If the structure does not change under pressure,  $L_c$  changes mainly due to the change of the density, and then  $L_c(P) \propto \rho(P)^{-1/3}$ . In this case from Eqs. (7) and (8) we have

$$\nu_{BP} = \nu_{0BP} \left( 1 + \frac{K_1}{K_0} P \right)^{\frac{\gamma_T + \frac{1}{3}}{K_1}}. \quad (9)$$

So, the boson peak frequency should change stronger with pressure than the Brillouin frequencies, with the exponent in Eq. (9) equal to

$$\frac{\gamma_T + \frac{1}{3}}{K_1} = k + \frac{1}{3K_1}. \quad (10)$$

This exponent is equal to 1/3 in the soft potential model. This prediction is reproduced if the Grüneisen parameter for Brillouin mode  $\gamma_T = 1.5$ . For polymers  $\gamma_T \sim 2-5$ . In polymers it was found that the exponent in Eq. (9) for boson peak is larger than 1/3, reaching values 0.5–0.6.<sup>18</sup> Such value of the exponent corresponds to  $\gamma_T \sim 2-3$  in Eq. (10). We note that the parameter  $b$  in Eq. (8) depends on the amplitude of spatial fluctuations of shear modulus on nanometer scale,<sup>19</sup> and so it may depend on pressure. In Ref. 20 it was shown that  $b$  increases if the amplitude of fluctuation decreases. That is what one can expect when applying pressure. Effectively, increase of  $b$  with pressure gives a positive contribution to the exponent in Eq. (9). Further study of the pressure dependence of the parameter  $A$  is needed, but in principle,

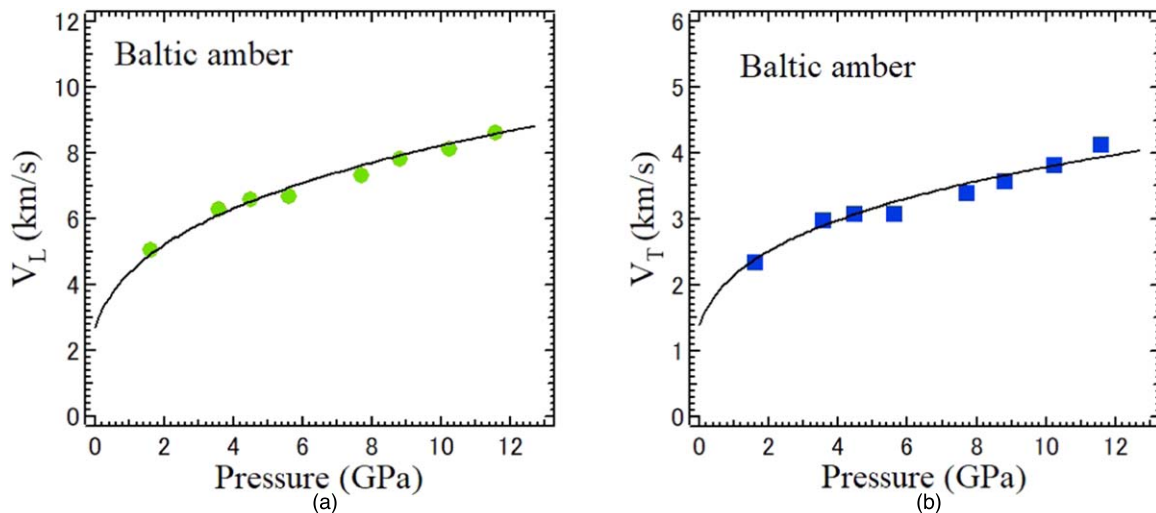


**Fig. 4.** (Color online) Pressure dependence of (a) LA and (b) TA sound velocities of Baltic amber. Solid lines in (a) and (b) are the fit by Eqs. (2) and (3), respectively.

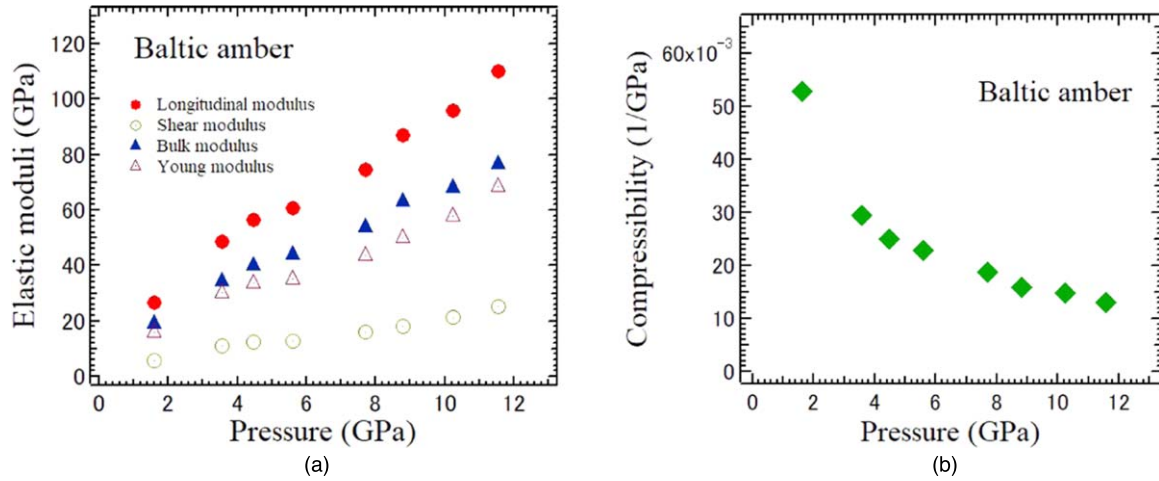


**Fig. 5.** (Color online) Pressure dependences of (a) longitudinal modulus, shear modulus, bulk modulus, Young's modulus, and (b) compressibility of Baltic amber.

the model (8) is capable to describe the pressure dependence of the boson peak frequency.

We note also, that according to the data of Fig. 5(a), the ratio  $K_0/K_1 \sim 2.2$  GPa. This value should be compared with  $P_0 \sim 0.25$  in the fitting functions (3) and (4). The deviation of  $P_0$  from the prediction of the simple model of Eq. (7) may mean that at such high pressures in amber the Grüneisen parameter depends on the pressure.

### 3.2. Elastic moduli at high pressures

The elastic properties are also sensitive to network structure of glasses. Since glasses are isotropic, following elastic constants are defined:

$$\text{Longitudinal modulus: } L = \rho V_L^2 \quad (11)$$

$$\text{Shear modulus: } G = \rho V_T^2 \quad (12)$$

$$\text{Young's modulus: } E = 2G(1 + \sigma) \quad (13)$$

$$\text{Bulk modulus: } K = L - \frac{4}{3}G \quad (14)$$

$$\text{Compressibility: } C = 1/K \quad (15)$$

$$\text{Poisson's ratio: } \sigma = \frac{1}{2} \frac{V_L^2 - 2V_T^2}{V_L^2 - V_T^2}. \quad (16)$$

The pressure dependences of longitudinal, shear, Young's, and bulk moduli, and compressibility are shown in Figs. 5(a) and 5(b), respectively. The longitudinal, shear, Young's, and bulk moduli show the remarkable increase, and compressibility shows the marked decrease with pressure increase.

The pressure dependence of the Poisson's ratio of Baltic amber up to 12.0 GPa is shown in Fig. 6. It is found that the Poisson's ratio  $\sigma$  of Baltic amber is nearly constant against pressure within experimental uncertainty. The elastic properties of three polymer elastomers, a cross-linked poly(dimethylsiloxane) (Sylgard®184), a cross-linked terpolymer poly(ethylene-vinyl acetate-vinyl alcohol), and a segmented thermoplastic poly(ester urethane) copolymer (Estane®5703), were measured up to 12 GPa by using Brillouin scattering.<sup>22)</sup> The pressure dependence of elastic properties of PEI, PES,

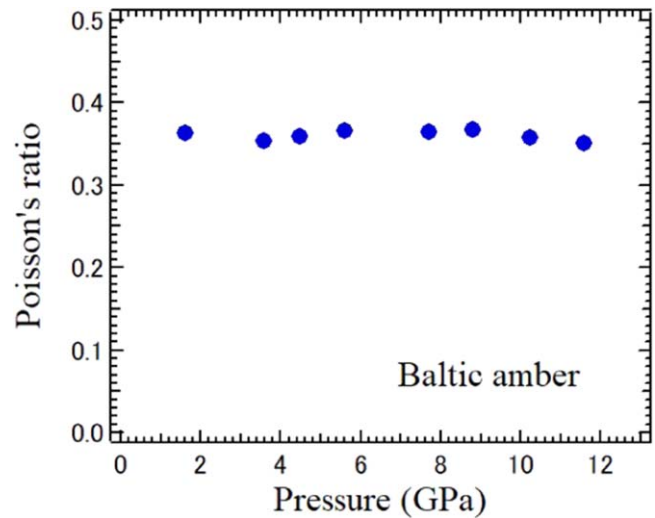


**Fig. 6.** (Color online) Pressure dependences of the Poisson's ratio of Baltic amber.

and PVC were also studied and similar results were reported. The pressure dependences of Poisson's ratio of these polymers are also very small and the values are close to that of Baltic amber.

Novikov and Sokolov have discovered that there exists a correlation between, the ratio of the bulk modulus  $K$  to shear modulus  $G$  and fragility  $m$  in various oxide and molecular glass systems.<sup>1)</sup> Park et al. formulated the correlation between fragility and Poisson's ration,  $\sigma = -0.179 + 0.312 \log m$ . They also suggested that the fragility should be approximately independent of pressure on the basis of the DDM.<sup>24,25)</sup> It may suggest that the Poisson's ratio is also approximately independent of pressure, and this fact is in agreement with the observed pressure dependence of Poisson's ratio in Baltic amber. Considering the correlation between fragility and Poisson's ratio, the fragility of amber may also remain constant value with pressure change.

### 3.3. Cauchy type relation of amber at high pressures

The number of independent elastic constants is only two, namely, the longitudinal ( $L$  or  $c_{11}$ ) and the shear ( $G$  or  $c_{44}$ ) modulus, where  $c_{11}$  and  $c_{44}$  are the elastic stiffness constants in isotropic systems. Additional local symmetry conditions

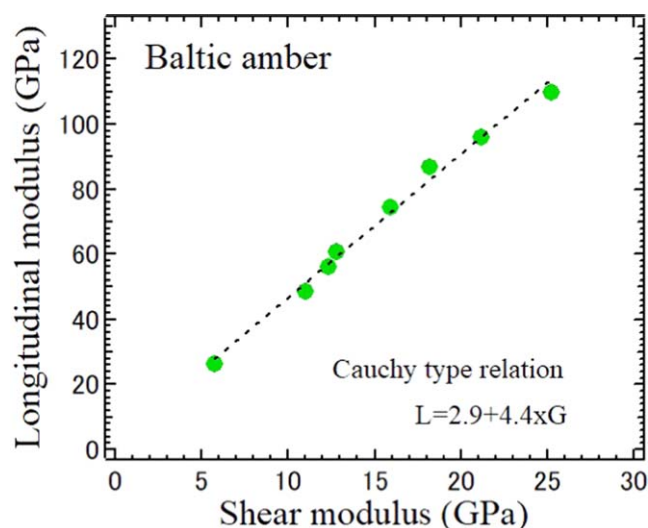


Fig. 7. (Color online) Cauchy type relation of Baltic amber at high pressures.

further reduce the number of independent elastic constants. The  $L/G$  ratio is an indicator of the character of the force field: if atoms interact through a central potential,  $L/G = 3$ , if through noncentral potential,  $L/G > 3$ . However, the most of glasses are far from central potential and Cauchy relation. The Cauchy-type relation  $L = A + BG$  ( $A$  is the material dependent constant) with  $B \approx 3$  was reported to hold for the high frequency limit values of  $L$  and  $G$  for some types of glasses.<sup>26)</sup> The high frequency limits values of  $L$  and  $G$  in the GHz range were determined by Brillouin scattering. Corezzi et al. reported the Cauchy-type relation for the time and temperature dependences of curing epoxy systems and thermal glass formers.<sup>27,28)</sup> For the compositional dependence of  $L$  and  $G$ , these values are  $A = 2.3$  GPa and  $B = 3.1$  for the alkali content dependence in the single alkali borate glasses.<sup>29)</sup> Philipp et al. studied the contribution of anharmonicity to the Cauchy type relation in the polymerization process of reactive polymers, and derived the equations for  $A$  and  $B$  using the elastic constants  $c_{11}$ ,  $c_{44}$ , and the Grüneisen parameters of TA and LA modes.<sup>30,31)</sup> Maczka et al. reported the Cauchy-type relation for the temperature dependence of  $M_2O$ – $MgO$ – $WO_3$ – $P_2O_5$  glasses ( $M = K, Rb$ ) glasses, in which  $A = 11.03$  GPa, 9.72 GPa and  $B = 2.67$ , 2.71 for K, Rb, respectively.<sup>32)</sup> The studied oxide glasses were characterized by relatively weak elastic anharmonicity in comparison with polymer glasses, that have higher fragility. Such difference obeys the correlation between the fragility and the Grüneisen parameters, since the anharmonicity increases as the fragility increases.<sup>33)</sup> Corezzi et al. discussed the breaking of boson peak scaling with respect to the time of reaction and temperature variation by the deviation from  $B = 3$ , and suggested that the deviation could be due to the development of long-range stresses in glasses.<sup>27)</sup>

The Cauchy type relation of Baltic amber for the pressure dependence is shown in Fig. 7. The fitting values are  $A = 2.9$  and  $B = 4.4$ . The deviation from  $B = 3$  is large in a Baltic amber. This implies higher fragility and the development of long-range stresses under high pressures. The Cauchy type relation of polymers for the pressure dependence up to 1.5 GPa was examined using the observed values from Ref. 21.<sup>27)</sup> The values of  $B$  for PS, PMPS, and PBD are

6.0, 5.6, and 4.6, respectively. This fact means that, for the pressure dependences, the values of  $B$  are usually much larger than 3 and the result for Baltic amber is normal for the pressure dependence in polymers.

The amber is basically a polymer of the labdatrienoid compounds, with addition of a few percent of other compounds such as succinic acid. The Cauchy relation,  $L/G = 3$ , holds for the interaction through a central potential that depends only on the distance  $r$  from the origin. The intermolecular interaction between the labdatrienoid compounds is the Van der Waals force expressed through a central potential. However, the intermolecular interaction of succinic acids with hydroxyl groups is the hydrogen bond. Its potential depends not only on interatomic distance but also on bond angle, and, therefore it is not a central one. It may be one of the origins of the deviation from the Cauchy relation in amber.

#### 4. Conclusions

Baltic amber is a natural polymer glass with high fragility index. Elastic properties of amber at high pressures have been studied using Brillouin scattering and a diamond anvil cell. Both LA and TA modes have been observed up to 12 GPa. The pressure dependences of longitudinal, shear, Young's, and bulk moduli, compressibility, and Poisson's ratio were determined. The longitudinal, shear, Young's, and bulk moduli show the remarkable increase, and compressibility shows the marked decrease with pressure increase. However, it is found that the pressure dependence of Poisson's ratio is very small. The mechanism of this small pressure dependence was discussed. The Cauchy type relation between longitudinal and shear moduli was examined. The obtained results suggest that the higher fragility and the development of long-range stresses under high pressures.

#### Acknowledgments

One of the authors, MA, acknowledges he received partial support from CDAC center (Chicago/DOE Alliance Center, DE-NA-0003858). The Advanced Photon Source is operated for the DOE Office of Science by Argonne National Laboratory under Contract No. DE-AC02-06CH11357. VNN acknowledges the support by the grant № 20-02-00314 of the Russian Fund for Fundamental Research.

#### ORCID iDs

Seiji Kojima  <https://orcid.org/0000-0003-1933-9269>

- 1) V. N. Novikov and A. P. Sokolov, *Nature* **431**, 961 (2004).
- 2) G. N. Greaves, A. L. Greer, R. S. Lakes, and T. Rouxel, *Nat. Mater.* **10**, 823 (2011).
- 3) A. Reiser and G. Kasper, *Eur. Phys. Lett.* **76**, 1137 (2006).
- 4) C. S. Zha, R. J. Hemley, H. Mao, T. S. Duffy, and C. Meade, *Phys. Rev. B* **50**, 13105 (1994).
- 5) S. Pawlus, M. Paluch, J. Ziolo, and C. M. Roland, *J. Phys.: Condens. Matter* **21**, 332101 (2009).
- 6) J. Zhao, E. Ragazzi, and G. B. McKenna, *Polymer* **54**, 7041 (2013).
- 7) J. S. Mills, R. White, and L. J. Gough, *Chem. Geol.* **47**, 15 (1984).
- 8) J. Zhao, S. L. Simon, and G. B. McKenna, *Nat. Commun.* **4**, 1783 (2013).
- 9) T. Sasaki, Y. Hashimoto, T. Mori, and S. Kojima, *Int. Lett. Chem. Phys. Astron.* **62**, 29 (2015).
- 10) T. Pérez-Castañeda, R. J. Jiménez-Riobóo, and M. A. Ramos, *Phys. Rev. Lett.* **112**, 165901 (2014).

- 11) C. H. Whitfield, E. M. Brody, and W. A. Bassett, *Rev. Sci. Instrum.* **47**, 942 (1976).
- 12) M. Ahart, F. Jang, and S. Kojima, *Jpn. J. Appl. Phys.* **37**, 2803 (1998).
- 13) S. N. Tkachev, M. Ahart, V. N. Novikov, and S. Kojima, *Proc. Symp. Ultrasonic Electron.* **41**, 3Pb1-2 (2020).
- 14) D. Fan, S. Fu, J. Yang, S. N. Tkachev, V. B. Prakapenka, and J.-F. Lin, *Am. Mineral.* **104**, 262 (2019).
- 15) K. H. Oh, Y. H. Ko, J.-H. Ko, and S. Kojima, *Proc. Symp. Ultrasonic Electron.* **40**, 1P1-3 (2019).
- 16) K. H. Oh, Y. H. Ko, S. Kojima, and J.-H. Ko, *J. Korean Phys. Soc.* **77**, 773 (2020).
- 17) A. Yoshihara, T. Maeda, and Y. Imai, *Vib. Spectrosc.* **50**, 250 (2009).
- 18) D. Quitmann, M. Soltwisch, and G. Ruocco, *J. Non-Cryst. Solids* **203**, 12 (1996).
- 19) V. L. Gurevich, D. A. Parshin, and H. R. Schober, *Phys. Rev. B* **71**, 014209 (2005).
- 20) S. Kojima, V. N. Novikov, M. Kofu, and O. Yamamuro, *J. Non-Cryst. Solids* **518**, 18 (2019).
- 21) L. Hong, B. Begen, A. Kisliuk, C. Alba-Simionesco, V. N. Novikov, and A. P. Sokolov, *Phys. Rev. B* **78**, 134201 (2008).
- 22) L. L. Stevens, E. B. Orler, D. M. Dattelbaum, M. Ahart, and R. J. Hemley, *J. Chem. Phys.* **127**, 104906 (2007).
- 23) K. H. Oh, Y.-H. Ko, and K.-J. Kim, *Physica B* **576**, 411722 (2020).
- 24) S. H. Glarum, *J. Chem. Phys.* **33**, 639 (1960).
- 25) E. S. Park, J. H. Na, and D. H. Kim, *Appl. Phys. Lett.* **91**, 031907 (2007).
- 26) R. Zwanzig and R. D. Mountain, *J. Chem. Phys.* **43**, 4464 (1965).
- 27) S. Corezzi, S. Caponi, F. Rossi, and D. Fioretto, *J. Phys. Chem. B* **117**, 14477 (2013).
- 28) S. Caponi, S. Corezzi, D. Fioretto, A. Fontana, G. Monaco, and F. Rossi, *Phys. Rev. Lett.* **102**, 027402 (2009).
- 29) S. Kojima, *Solids* **1**, 16 (2021).
- 30) J. K. Krüger, J. Baller, T. Britz, A. le Countre, R. Peter, R. Bactavatchalou, and J. Schreiber, *Phys. Rev. B* **66**, 12206 (2002).
- 31) M. Philipp, C. Vergnat, U. Müller, R. Sanctuary, J. Baller, W. Possart, P. Alnot, and J. K. Krüger, *J. Phys.: Condens. Matter* **21**, 035106 (2009).
- 32) M. Maczka, J. Hanuza, J. Baran, A. Hushur, and S. Kojima, *J. Chem. Phys.* **125**, 244503 (2006).
- 33) S. Kojima, V. Novikov, and M. Kodama, *J. Chem. Phys.* **113**, 6344 (2000).